Design, Implementation and Control of Dual Axis Self Balancing Inverted Pendulum using Reaction Wheels

Abdullah Türkmen[1], M. Yusuf Korkut[1], Mustafa Erdem[1], Ömer Gönül[2], and Volkan Sezer[3]

[1]Mechatronics Graduate Program, Istanbul Technical University, Istanbul, TURKEY
turkmenab@itu.edu.tr, korkutmu15@itu.edu.tr, erdemm@itu.edu.tr
[2]Energy Institute, Istanbul Technical University, Istanbul, TURKEY
gonulo@itu.edu.tr
[3]Dept. of Control and Automation Engineering, Istanbul Technical University, Istanbul, TURKEY
sezerv@itu.edu.tr

Abstract

Inverted pendulum systems have an important place in practice for control problems due to their nonlinear structures. It is a very difficult task to control the orientation and speed of objects and robots which are free in three dimensions. These systems constitute the substructure of many advanced systems. Conventional actuators may not be used in such applications due to various limitations. Under these circumstances usage of reaction wheels come into prominence. Reaction wheel based systems are used for orienting, coordinating and balancing of spacecraft, transport systems, and other such systems. In this study, dual axis self-balancing reaction wheel based inverted pendulum system which is a basis for many complex systems has been designed, manufactured and controlled.

1. Introduction

Many studies have been done about inverted pendulum and reaction wheel based inverted pendulum systems. In [1], a study about linear control of reaction wheeled inverted pendulum has been done. In [2], a study about nonlinear control of inverted pendulum in two axes has been done. A study of fuzzy logic based control has been done in [3]. Spong et al. have done modelling and control studies on reaction wheel based systems in [4].

Reaction wheels can apply torque to the body they are attached by using the inertia of a rotating wheel and by this means they can change the orientation of the body. Inverted pendulum systems have a very rich background [5] and they are frequently used for testing, implementing and comparing new control concepts and theories [6]. The most significant difference between the proposed system and existing classical inverted pendulum systems is the use of reaction wheels in order to achieve balance.

In general, reaction wheels are used to control the orientation of space crafts in space which has no gravitation and no friction without using rocket fuel or any other actuator. The basic working principle is based on the Newton's third law: "For every action, there is an equal and opposite reaction."

Based on these, a reaction wheel attached to any motor creates a momentum which is equal and opposite to the angular momentum that has been generated because of the law of conservation of momentum depending on its angular velocity. Reaction wheels can only generate momentum around their center of mass. Therefore, they cannot generate translational motion.

Just like any other system, the angular momentum will be conserved if no external torque is applied. Therefore, by applying counter torques to falling direction with reaction wheels, the system can be balanced. The motors that are controlled for this purpose have balanced the pendulum around the point that the pendulum is touching the ground.

2. System Modeling

The two axes of the system are considered to be independent of each other and the motion equations are derived for a single axis. For this purpose, system considered as in Figure 1 and modeled by Lagrange method.

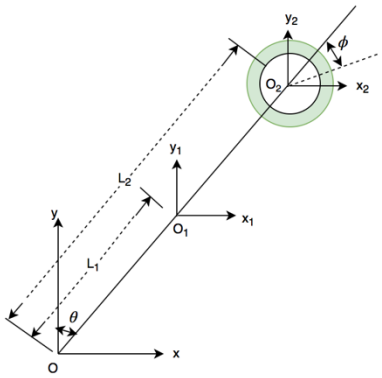

Fig. 1. Single axis inverted pendulum with reaction wheel model

- O_1 center of gravity of pendulum
- O_2 center of gravity of reaction wheel
- L_1 distance between origin(O) and the center of gravity of pendulum
- L_2 distance between origin(O) and the center of gravity of reaction wheel
- θ angle between pendulum and vertical axis
- ϕ angle of reaction wheel

General Lagrange expression is given in (1).

$$\frac{d}{dt}\left(\frac{\partial \mathcal{L}}{\partial \dot{q}_i}\right) - \frac{\partial \mathcal{L}}{\partial q_i} = \tau_i \qquad (1)$$

Here $\mathcal{L}$ is the Lagrance operator, q_i are generalized coordinates (for our system θ and ϕ), τ_i are the total torques of these coordinates. Lagrange operator is defined as the difference between kinetic and potential energy as it is shown in (2).

$$\mathcal{L} = KE - PE \tag{2}$$

- KE : Total kinetic energy of the system
- PE : Total potential energy of the system

Kinetic and potential energy expressions of the system are given in Equation (3) and (4).

$$KE = \frac{1}{2}(m_1L_1^2 + m_2L_2^2 + I_1 + I_2)\dot{\theta}^2 + I_2\dot{\theta}\dot{\phi} + \frac{1}{2}I_2\dot{\phi}^2 \tag{3}$$

$$PE = (m_1L_1 + m_2L_2)gcos\theta \tag{4}$$

- m_1 mass of pendulum
- m_2 mass of reaction wheel
- I_1 moment of inertia of pendulum around center of gravity
- I_2 moment of inertia of reaction wheel around its center of gravity

We obtain the Lagrange operator as in (5), after writing the Equations (3) and (4) into (2).

$$\mathcal{L} = \frac{1}{2}(m_1L_1^2 + m_2L_2^2 + I_1 + I_2)\dot{\theta}^2 + I_2\dot{\theta}\dot{\phi} + \frac{1}{2}I_2\dot{\phi}^2 - (m_1L_1 + m_2L_2)gcos\theta \tag{5}$$

For both coordinates, we obtain the (6) and (7) after writing Equation (5) in Equation (1).

$$(m_1L_1^2 + m_2L_2^2 + I_1 + I_2)\ddot{\theta} + I_2\ddot{\phi} - (m_1L_1 + m_2L_2)gsin\theta = 0 \tag{6}$$

$$I_2(\ddot{\theta} - \ddot{\phi}) = T_r \tag{7}$$

Here T_r is the reaction wheel drive torque without considering friction and electrical dynamics of DC motor. Equation (6) can be rewritten as in (8) after linearization. Since $sin(\theta)$ is the only non-linear element in the equations, Equation (7) is not changed.

$$(m_1L_1^2 + m_2L_2^2 + I_1 + I_2)\ddot{\theta} + I_2\ddot{\phi} - (m_1L_1 + m_2L_2)g\theta = 0 \tag{8}$$

In the next step, to control the reaction wheel at the desired speed the mathematical model of the motor's physical behavior was included in the system with Equations (9), (10) and (11).

$$V = L_m\frac{di}{dt} + R_mi + K_e\omega_m \tag{9}$$

$$T_m = K_ti \tag{10}$$

$$T_r = N_gT_m \tag{11}$$

Variables in these equations defined as the following: V motor voltage, K_e motor back electro-magnetic force, ω_m angular velocity of the motor, L_m armature coil inductance, R_m armature coil resistance, i armature current, T_m motor generated torque, K_t motor torque constant and N_g gear ratio. Since the inductance of the motor relatively less than its resistance ($L_m \ll R_m$), we neglect the inductance term in the equation. Using the relationship between the motor and the reaction wheel, we can calculate the required motor voltage in terms of the reaction wheel angular velocity as in (12):

$$T_r = N_gK_t\left(\frac{V - K_eN_g\dot{\phi}}{R_m}\right) \tag{12}$$

After all these steps state-space representation of the system obtained as in Equation (13) and (14).

$$\begin{bmatrix}\dot{\theta}\\ \ddot{\theta}\\ \dot{\phi}\\ \ddot{\phi}\end{bmatrix} = \begin{bmatrix}0 & 1 & 0 & 0\\ a_{21} & 0 & 0 & a_{24}\\ 0 & 0 & 0 & 1\\ a_{41} & 0 & 0 & a_{44}\end{bmatrix}\begin{bmatrix}\theta\\ \dot{\theta}\\ \phi\\ \dot{\phi}\end{bmatrix} + \begin{bmatrix}0\\ b_2\\ 0\\ b_4\end{bmatrix} \tag{13}$$

$$y = \begin{bmatrix}1 & 0 & 0 & 0\end{bmatrix}\begin{bmatrix}\theta\\ \dot{\theta}\\ \phi\\ \dot{\phi}\end{bmatrix} \tag{14}$$

As it can be noticed, to write the state-state representation in a more compact form following variables were defined.

$$a = m_1L_1^2 + m_2L_2^2 + I_1\,,\, b = (m_1L_1 + m_2L_2)g,$$

$$a_{21} = \frac{b}{a}\,,\, a_{24} = \frac{K_tK_eN_g^2}{aR_m}\,,\, a_{41} = -\frac{b}{a},$$

$$a_{44} = \left(\frac{a + I_2}{aI_2}\right)\left(\frac{K_tK_eN_g^2}{R_m}\right),$$

$$b_2 = -\frac{K_tN_g}{aR_m}\,,\, b_4 = \left(\frac{a + I_2}{aI_2}\right)\left(\frac{K_tN_g}{R_m}\right)$$

3. Mechanical Design

The 3D design has been done in computer environment using SolidWorks. During development of the design, existing designs in the literature have been used [2], because there were no specific physical requirements. However, minor changes in design of reaction wheels have been done in order to minimize weight without compromising the inertia. Manufacturability of the parts have been considered. The design consists of 2 reaction wheels, 2 assembly apparatuses that are used to attach the wheels to motors, 2 motor holders, a rod that forms the main body of the pendulum, a main holder that ties motor holders to the rod, a tip that is attached to bottom of the rod to touch the ground and an IMU holder at the top of the rod.

The design of the reaction wheel is given in Figure 2 which is an important part of the system. They are manufactured from aluminum, have a diameter of 70 mm and weight 42 grams.

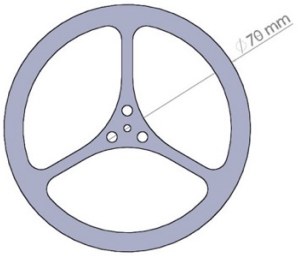

Fig. 2. Reaction wheel CAD drawing

An aluminum motor holder given in Figure 3 is designed in order to attach motors to the pendulum body. The rod has been cut from an aluminum tube in a way that the rod has a height of 30 cm, has an outer diameter of 9 mm and has an inner diameter of 7 mm. All of other aluminum parts are manufactured with the use of CNC milling machine.

Completed design and CAD model of the overall system is given in Figure 4 and a picture of the manufactured system is given in Figure 5.

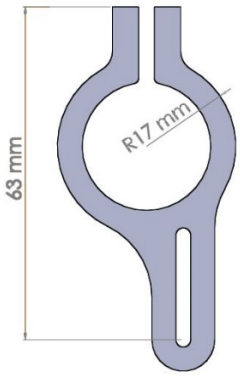

Fig. 3. Motor holder CAD drawing

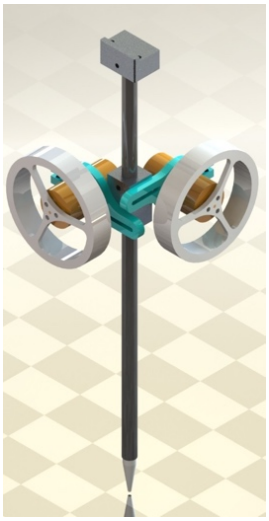

Fig. 4. System CAD drawing

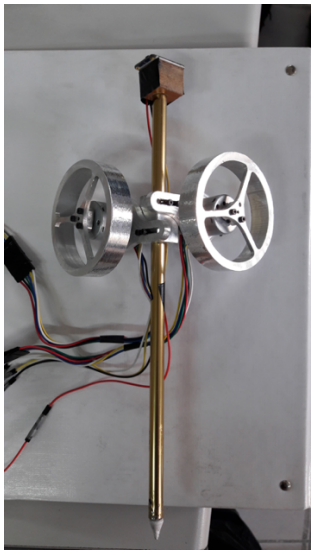

Fig. 5. Manufactured system

4. Electronic Structure of System and Communication

The system includes: two 12V gearless DC motor, motor driver which amplifies the appropriate control signals for the motors and inertial measurement unit (IMU) that measures the necessary angle values for the system. The control algorithms of the system are coded by using Arduino interface and embedded to Arduino Mega board. To communicate the Arduino board with the computer, a user interface that has a capable of serial communication is designed via Visual Studio program with C# language as shown in Figure 6.

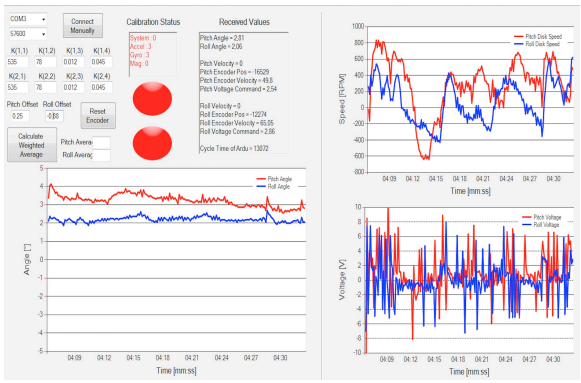

Fig. 6. User interface

5. Control and Simulations

For the control of the mathematical model obtained system, pole placement technique is used. The applicable methods in classical PID method are more restricted than the pole placement technique due to not being fed back of all system states. In pole placement technique, closed loop poles of the system can be shifted systematically to desired locations with the state feedback gain matrix.

The general scheme of the closed loop state feedback system with pole placement technique is as shown in Figure 7.

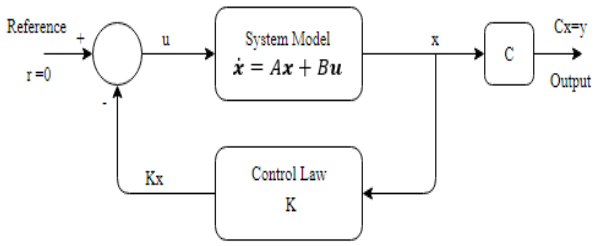

Fig. 7. General scheme of state feedback control system

The state space representations of the continuous time systems are defined as in (15) and (16) where x, y and u represent state matrix, output matrix and input respectively;

$$\dot{\boldsymbol{x}} = A\boldsymbol{x} + B\boldsymbol{u} \tag{15}$$

$$y = C\boldsymbol{x} + D\boldsymbol{u} \tag{16}$$

For our designed system, the A, B, C and D matrices are as shown in (17) and (18);

$$A = \begin{bmatrix} 0 & 1 & 0 & 0 \\ 49.7 & 0 & 0 & 0.0026 \\ 0 & 0 & 0 & 1 \\ -49.7 & 0 & 0 & 0.8165 \end{bmatrix} \quad B = \begin{bmatrix} 0 \\ -0.2337 \\ 0 \\ 72.71 \end{bmatrix} \tag{17}$$

$$C = \begin{bmatrix} 1 & 0 & 0 & 0 \\ 0 & 1 & 0 & 0 \\ 0 & 0 & 1 & 0 \\ 0 & 0 & 0 & 1 \end{bmatrix} \quad D = \begin{bmatrix} 0 \\ 0 \\ 0 \\ 0 \end{bmatrix} \tag{18}$$

Here, control rule is defined as with the state feedback gain matrix $\boldsymbol{u}$= -$K\boldsymbol{x}$ and then the state equation in (15) is written as in (19);

$$\dot{\boldsymbol{x}} = A\boldsymbol{x} - BK\boldsymbol{x} = (A - BK)\boldsymbol{x} \tag{19}$$

Using (19) and desired pole locations, the state feedback gain matrix is calculated by (20).

$$|sI - A + BK| = (s - s_1)(s - s_2) \dots (s - s_n) \tag{20}$$

$s_1, s_2, \dots, s_n$ represent the desired pole locations of the system. These values are tried to be optimized on simulation and real time system by trial and error. The closed loop system poles are selected as s_1= -4, s_2= -3, $s_{3,4}$= -1.2±0.25j and with these values, the K matrix is found as in (21).

$$K_e = [-438.7 \quad -58.04 \quad -0.005 \quad -0.046] \tag{21}$$

- K_e: The state feedback gain matrix obtained according to Lagrange method based mathematical model

The system is simulated with calculated K_e matrix with 0.01 radian initial system start condition as in Figure 8. It is observed that the system can balance itself successfully.

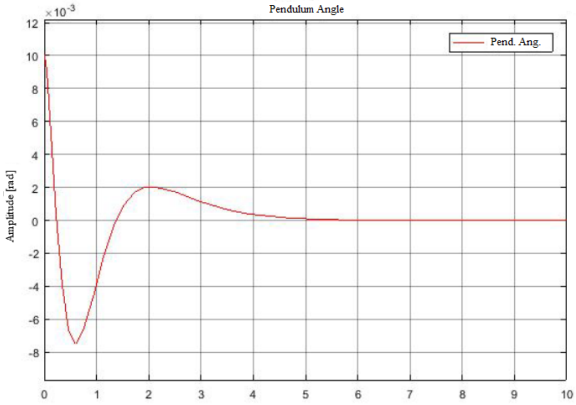

Fig. 8. System simulation with Ke via pole placement

6. Experiments

Derived mathematical model was first simulated by the pole placement method and then the obtained parameters were tested on the real system.

Figure 9 shows the pitch and roll angles when K_e applied on the system and Figure 10 shows the absolute error of these angles. Equation (22) is the formula that is used to calculate the absolute error.

$$\overline{Error}_{angle} = \left| \sum_{i=1}^{n} \frac{angle_i - angle_{average}}{n} \right| \tag{22}$$

n represents number of data samples that we collected while system is working.

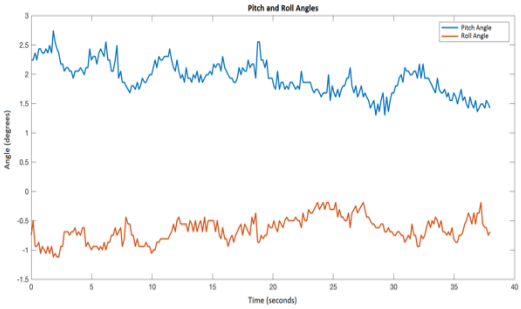

Fig. 9. Pitch and roll angle of pendulum

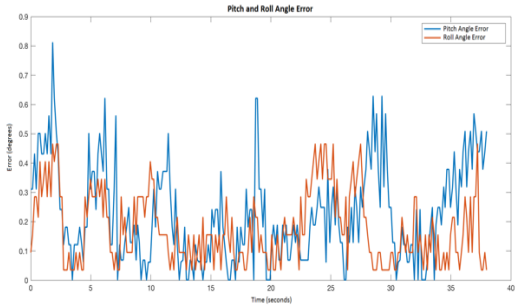

Fig. 10. Pitch and roll angle error of pendulum

Since the center of gravity is not on the pendulum, pitch and roll angles do not converge to zero but instead softly oscillate around a constant value.

As it can be seen from Figure 10, error values increase and decrease from time to time but never constantly change in same direction. It is also possible to understand from this that the system can successfully balance itself. In recent experiments, average error values calculated as 0.22 degree for pitch angle and 0.17 degree for roll angle. A picture of the working system is shown in Figure 11 as an exemplary.

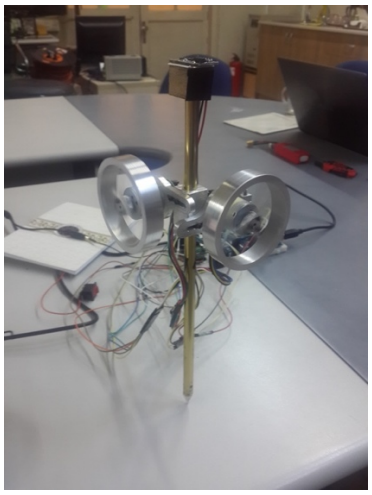

Fig. 11. Exemplary picture of balanced reaction wheel based inverted pendulum

7. Conclusions

In this study, reaction wheel based dual-axis inverted pendulum system has been successfully implemented. At first, system modeled by using Lagrange method. After that, some approximations were made with the help of simulations to determine the system's criteria and continue with the material supply and production stage. The pole placement method has been chosen as the control strategy of the system. In future studies, we are planning to apply different control methods on the system and compare their results.

8. Acknowledgement

This work is done within the Mechatronics System Design course and is supported by Istanbul Technical University – Mechatronics Education and Research Center. Also, we would like to extend our sincere thanks to Assoc. Prof. Dr. Erdinç Altuğ who gives us opportunity to practice in Autonomous Systems Laboratory of Department of Mechanical Engineering.

9. References

[1] M. Olivares, P. Albertos, "Linear control of the flywheel inverted pendulum", ISA Transactions 53 (2014), pp. 1396-1403

[2] L.H. Chang, A.C. Lee, "Design of nonlinear controller for bi-axial inverted pendulum system", IET Control Theory Appl., (2007), pp. 979-986

[3] X. Ruan, Y. Wang, "The modelling and control of flywheel inverted pendulum system", 3rd IEEE International Conference on Computer Science and Information Technology (ICCSIT) (2010)

[4] D.J. Block, K.J. Astrom, and M.W. Spong, "The Reaction Wheel Pendulum", Morgan & Claypool Publishers

[5] A. Stephenson, "On a new type of dynamical stability," Proceedings: Manchester Literary and Philosophical Society, vol. 52, pp. pp. 1-10, 1908.

[6] P. Reist and R. Tedrake, "Simulation-based lqr-trees with input and state constraints," in Robotics and Automation (ICRA), 2010 IEEE International Conference on, may 2010, pp. 5504-5510.